Università degli Studi di Napoli Federico II

Dottorato di Ricerca in Scienze Veterinarie XXIX° ciclo

Polymer bioactivation: a versatile tool to guide angiogenesis and tissue regeneration

Maria De Gregorio

Coordinator
Prof. Giuseppe Cringoli

Advisor
Prof. Paolo Netti
Phd. Chiara Attanasio

2014-2017

Contents

Abbreviations

TE	Tissue Engineering
ECM	Extracellular matrix
ECs	Endothelial cells
HUVECs	Human umbilical vein endothelial cells
PLA	Polylactic acid
PGA	Poly (glycolic acid)
PLLA	Poly-L-lactic Acid
PCL	Poly (lactic-co-glycolic acid)
HA	Hyaluronic acid
VEGF	Vascular endothelial growth factor
FGF	Fibroblast growth factor
RGD	Arginylglycylaspartic acid
SEM	Scanning electron microscope
Cryo-TEM	Cryogenic transmission electron microscopy
NOA63	Norland optical adhesive
ROI	Rectangular regions of interests
PFA	Paraformaldehyde
SHG	Second harmonic generation
pDR1m	Ppoly (Disperse Red 1 methacrylate)
PHTx	Partial hepatectomy
CORMs	CO-releasing molecules
Mb	Myoglobin
MbCO	Deoxy-myoglobin
NPs	Nanoparticles

Outline of the thesis

This PhD thesis stems from a project developed at the Center for Advanced Biomaterials for Health Care/CRIB Istituto Italiano di Tecnologia in Naples (Italy). The aim of the project is to enhance the ability of bioactive polymeric matrices to guide regeneration through a spatial and temporal control of angiogenesis. In this context I was mainly focused on studying the performance of engineered constructs from a biological standpoint. I was also involved in multidisciplinary activities including scaffold, biomaterial and nanocarrier design and fabrication.

Aiming to guide angiogenesis in a space and time controlled fashion we produced scaffolds with controlled porosity suitable to be loaded with vascular growth factors in order to generate a biochemical gradient. To this purpose the constructs were fabricated using two different assembly techniques: the random one, which implies an uncontrolled porosity, and the ordered one, which allows to control porosity features. Afterwards, I investigated the interplay between the scaffold and the cells, as well as the host tissue, after implantation. Several biological processes are mediated by biochemical signals, or rather by gradients of these signals, which precise regulation is essential for the physiological function of tissues and organs. These gradients, besides the direction also affect the rate of cellular invasion as well as the onset of the vascular network. A number of studies show that endothelial cells are particularly influenced by extracellular matrix topography.

Therefore, we decided to investigate if these signals are able to guide sprouting angiogenesis in a space and time controlled manner without the use of growth factors. To this aim we used a photoswitch-based strategy to modify the biomaterial surface, through a reversible photochemical technique, in order to resemble physiological dynamic signals. This part of the thesis project was developed through an internal collaboration within the IIT@CRIB with Dr. Silvia Cavalli and Dr. Chiara Fedele.

Finally, since in the past I was involved in studies focused on the therapeutic use of Carbon Monoxide (CO) to restore organ function after ischemia/reperfusion injury, I hypothesized that the advantages related to the use of polymer nanocarriers may contribute to solve the open challenges related to the use of this gas in the clinical practice. These issues are mostly related to the administration of CO, specifically to the possibility to get therapeutic concentrations of carboxyhaemoglobin in the blood without inducing toxicity.

Thus, in order to expand my skills, I spent few months at the Center for Life Sciences of Beth Israel Deaconess Medical Center at Harvard Medical School (Boston, MA, USA) where I had

the possibility to work in a very stimulating environment under the supervision of Prof. L. E. Otterbein the key scientist exploring the therapeutic properties of CO.

Chapter 1

Introduction

1.1.1 Tissue engineering: an overview

The partial or total loss of organs and tissues is a major cause of hospitalization in the world (1). Despite the progress made in the field of regenerative medicine, transplantation still remains the only option for several degenerative diseases when a substitutive therapy is not available (2).

However, it still suffers from a number of limitations that reduce its success. First of all, the shortage of organ donors, and then the need of a lifelong immunosuppressive therapy, the risk of infection at the graft site and other complications such as haemorrhages, fistulas, thrombosis and rejection. All these hindrances have led to the development of a new science: tissue engineering (TE), that has quickly become a key research area in the field of regenerative medicine (1-3).

TE is a multidisciplinary science that includes the principles of chemistry, biochemistry, medicine, engineering and physics, aiming to provide engineered tissues to restore the lost function of damaged tissues and organs (4).

This discipline combines scaffolds, cells and biologically active molecules to build functional tissues. The ability of an engineered construct to resemble the structural and functional properties of the damaged tissue is of basic importance to determine the success or the failure of its implantation in the host (5).

1.1.2 Cell-material interaction

Cells are the "building blocks" of all tissues, which are the basic functional units of the body. However, cells are unable to accomplish their function if the surrounding microenvironment is inadequate (6). Tissues, indeed, are made-up of two basic components: the cells and the extracellular matrix (ECM). The latter plays a key role in providing mechanical support to the cells but also including signal molecules which are critical for cell function.

By understanding how cells respond to these signals, interact with the surrounding microenvironment and organize themselves into tissues and organs, researchers worldwide are becoming able to direct cell fate and to restore the original function of damaged tissues, even creating new ones. In order to design a novel biomaterial, one of the most important features to consider is the so called cell-material interaction, that is the potential interplay between the material surface and the cell.

The biochemical and biophysical characteristics of a biomaterial, indeed, directly influence cell behaviour, for example by triggering specific events such as cell adhesion, migration, proliferation and differentiation (7). The interaction of biological systems with synthetic material surfaces is, therefore, a critical issue for biological applications of implantable devices and engineered tissues (8).

To collect reliable data, the main challenge is the design and the development of a surface able to interact with both biomolecules and cells without altering cell function and phenotype (9).

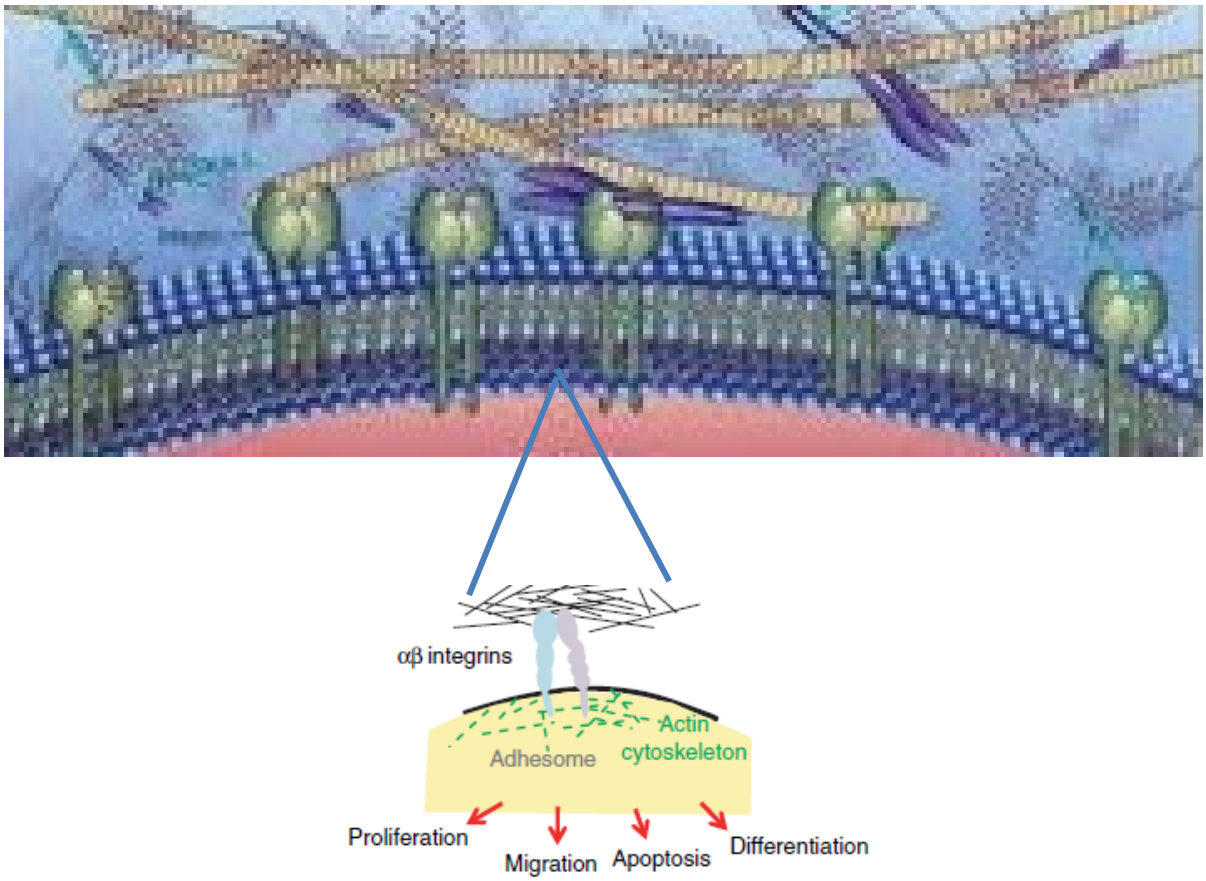

Figure1. The image shows the influence of ECM signals in the induction of critical events such as cell proliferation, migration and differentiation *(Francisco M. et al, Human gene therapy methods, 2013; 24:160-170).*

1.1.3 Biomaterial properties

A biomaterial is a natural or synthetic material able to be used for biomedical applications. There are several classes of biomaterials ranging from organic polymers to metals and glass (10). All of them have to fulfil essential requirements in terms of biocompatibility, biodegradability and functionality.

More in details, the first feature is the ability of the material to integrate with the host tissue without adverse effects (rejection, inflammation or toxicity), the second is the ability to be degraded through the enzymatic reactions that take place in the body, while the third refers to the physical and mechanical properties that devices and constructs should have in order to replicate the function of the damaged tissue.

A key point for many biomaterial applications is the interplay between the material and the biological environment after implantation, in particular at tissue/material interface. (5). Synthetic biodegradable polymers approved by the Food and Drug Administration are currently chosen by several research groups as scaffolding polymers. However, they have a main drawback consisting in the lack of specific cellular signals.

The most widely used synthetic polymers are biodegradable polyesters such as polyglycolic acid (PGA), polylactic acid (PLA) and polycaprolactone (PCL). The latter is made of five non-polar methylene groups and a relatively polar ester group. This structure implies a very slow degradation kinetic compared to those of PLA and PGA that enables PCL to deliver drugs for more than one year (11).

In addition, a scaffold has to display specific mechanical properties, such as elasticity and resistance that enable it to tolerate the physiological load over time after implantation (12). The ideal scaffold must also display a highly porous structure. Pores interconnection, indeed, is a prerequisite for a uniform cell distribution throughout the construct as well as for cell survival, proliferation and migration (13).

Further, these features are the basis for a homogeneous neovascularization of both the scaffold and the surrounding tissues after implantation. Scaffold pore size should be at least 100-200 μm in diameter in order to support an adequate diffusion of oxygen and nutrients as well as waste removal (14).

1.1.4 The angiogenesis cascade

Angiogenesis, the formation of new blood vessels from existing ones, occurs only during post-natal life, both in physiological and pathological conditions, for example wound repair in the first case and neoplastic events or inflammation in the second one (16).

The process is triggered by stimuli related to the secretion of specific growth factors, first of all vascular endothelial growth factor (VEGF), but also fibroblast growth factor (FGF) and angiopoietin, acting as triggers in response to hypoxia. In hypoxic conditions, indeed, the low oxygen level induces the formation of a new vascular network to support cellular metabolism (17). Several steps are involved in the process (Figure 2): 1) degradation of the basement membrane by proteolytic enzymes secreted by endothelial cells; 2) endothelial cell proliferation; 3) duct formation and branching; 4) development of vascular loops; 5) stabilization and functional maturation of

newly formed vessels, including the perivascular component and pericytes; 6) synthesis of basal membrane constituents (18).

When oxygen supply to the tissue becomes sufficient, growth factors are down-regulated while synthesis and release of angiogenesis inhibitors increase (19). Porous scaffolds generally allow the onset of a newly formed vascular network however, this is often composed of irregular and tortuous vessels causing a dramatic alteration of blood flow with increased vascular permeability and thrombi formation (20).

In addition, an insufficient vascularization leads to tissue ischemia and, in turn local wounds and organ damage (21). Further, the vascularization of an implanted scaffold is often too slow or limited to its surface implying scarce nutrients supply followed by implant failure (22).

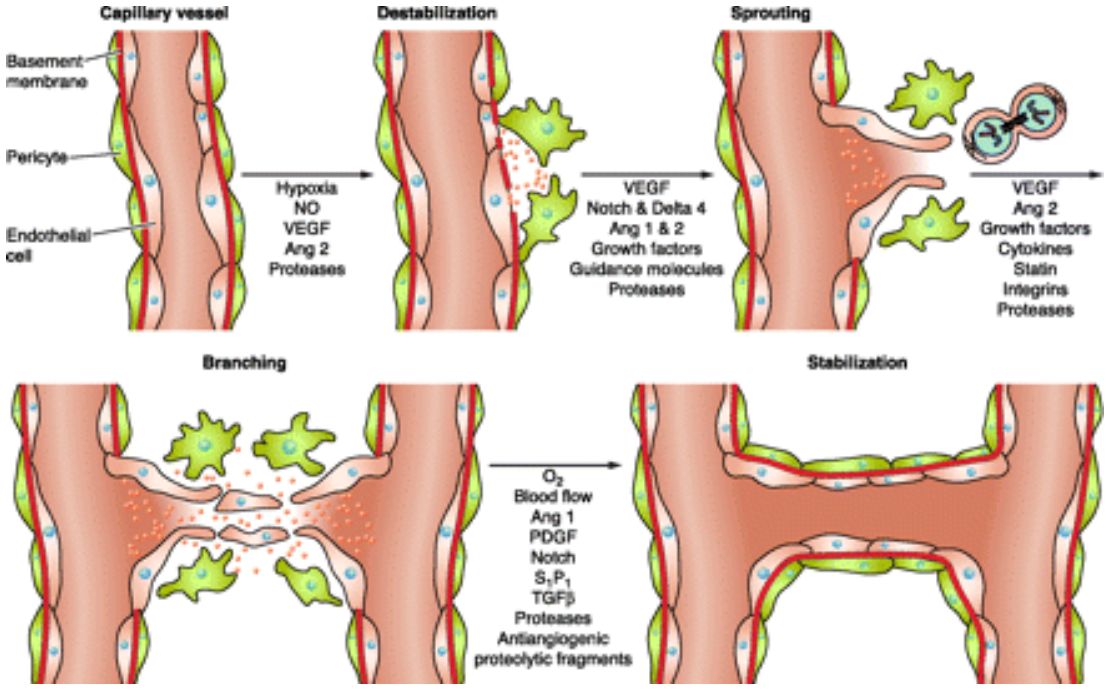

Figure 2. Steps involved in the angiogenic process. Hypoxia induces the production of proteases to increase the permeability of the capillary vessel wall that allows endothelial cells to migrate, proliferate and form tubules. Maturation of the newly formed tubules is associated with an increased expression of antiangiogenic factors (*Clappat C. et al., Physiol Rev. 2009; 1177-1215).*

Chapter 2

A bioactive bottom-up scaffold to guide angiogenesis

2.1.1 Promoting angiogenesis in tissues engineering

Theoretically, cells seeded on/onto biomaterials are able to create functional tissues. A critical point, however, is how to provide adequate oxygen and nutrients supplies to the inner part of the construct in order to support cell survival and proliferation as well as the integration of the developing tissue with the host one. Rapid revascularization of the damaged tissue through the implantation of polymeric matrices is essential (23). Polymers used to fabricate scaffolds suitable to be invaded by newly formed vessels may be natural or synthetic. Among natural materials commonly used there are hyaluronic acid (HA), collagen, fibrin, and alginate that, after subcutaneous implantation, may induce a little inflammatory response (24-25-26). Some examples of synthetic materials are poly (glycolic acid) (PGA), Poly-L-lactic Acid (PLLA) and copolymers such as PLGA. These materials enable the modulation of various parameters, including surface features and porosity degree.

To encourage cell adhesion to biomaterials the tripeptide Arginylglycylaspartic (RGD) sequence is commonly used. In fact, RGD-peptide, being a part of fibronectin molecule, mediates cell attachment by interacting with cellular integrins. Therefore it is used in the coating of synthetic scaffolds for tissue engineering in order to facilitate cell attachment by mimicking physiological cues (27).

Scaffolds alone are able to support vascular infiltration to enhance wound repair while, when loaded with growth factors, they can be used for controlled delivery of proangiogenic molecules (24). The methods commonly used to load angiogenic factors into the scaffold are: adsorption (25), encapsulation (26), entrapment or covalent binding (27). The last three mechanisms enable a controlled release of the molecules, however during scaffold manufacturing the bioactivity of these molecules may be affected. In order to overcome this issue growth factors may be adsorbed on the scaffold surface. Adsorption is achieved by exploiting ionic or hydrogen bonds as well as

Van der Waals or hydrophobic forces. These interactions are non-covalent and, in turn, weak causing a quick and uncontrolled release of the adsorbent protein.

Concerning scaffold fabrication techniques over the years two different approaches have been developed: top-down or conventional technique and bottom-up or unconventional technique. There are several top-down methods that, through a series of chemical reactions or physical modifications, lead to the development of a bulk material displaying a given structure with the desired characteristics.

Traditional technologies include solvent casting, gas foaming and phase separation, to name a few. The main downside of these techniques is scaffold architecture, which fails to mimic the extracellular matrix. In contrast, the bottom-up approach is based on a computer-assisted assembly of small blocks, which enables a better control of the polymer matrix structure organization

2.2 Materials and methods

2.2.1 Poly(ε-caprolactone) microsphere production

PCL microspheres were made by a single oil-in-water emulsion technique. The polymer (10% w/v) was dissolved in dichloromethane (DCM Romil Pure Chemicals). An aqueous solution of bidistilled water with 0.5% of polyvinyl alcohol (PVA) (100 ml Sigma-Aldrich PVA 4088 MW = 13-23 kDa, 87-89% hydrolyzed) and Tween 21 (100 μL) was placed under magnetic stirring at a temperature around 100 °C in order to completely dissolve the emulsifying agent (PVA), which is essential to reduce coalescence. The polymer solution was added dropwise to the aqueous phase and stirred for 3 hours at 500 rpm using a mechanical stirrer.

Microspheres were then isolated by three washing cycles in distilled water and filtered in order to completely remove the PVA (28-29). Afterwards they were sieved with a commercial sieve (Sieve IG / 3-EXP) to select microspheres with a 425-500 μm diameter .

2.2.2 Fabrication of Poly (lactic-co-glycolic acid) microspheres loaded with QK

PLGA (Resomer® RG 504H) microspheres containing QK were prepared with the multiple emulsion water/oil/water (W/O/W) technique. A sterile water solution containing QK (250 µl) was emulsified through homogenization at 8000 rpm for 1 minute in a solution containing 2.5 ml of PLGA and poloxamer 188 (ratio 5: 1) in dichloromethane (10% w/v). Poloxamer is a polymer with surfactant properties used to protect PLGA microsphere surface during the fabrication process.

The emulsion obtained was then added to the aqueous solution containing PVA (1.5% w/v) (Mowiol® 40-88) and emulsified with an electronic shaker at 450 rpm for 3 hours at room temperature, in order to allow solvent evaporation. Afterwards, the microspheres were washed in 30 ml of distilled water by centrifugation at 5000 rpm for 10 minutes at 4°C (three times) and lyophilized through a 24-hour cycle (0.001 atm, -60 °C).

2.2.3 Scaffold assembly

Scaffolds of 5x5 mm length and 1,5 mm height were assembled by using the sintering technique, that allowed a partial dissolution of their surface enabling the creation of three-dimensional porous structures. During this partial dissolution the microspheres developed the connections between each other. For ordered scaffold fabrication microsphere monolayers were arranged into a mold of polydimethylsiloxane (PDMS). Afterwards 100 ml of anisole were poured over the microspheres in order to induce a moderate swelling and, in turn, the development of sintering necks. We chose anisole because this solvent, due to its low toxicity, is considered ideal for the fabrication of constructs for in vivo applications (3). After the exposure to anisole for 5-10 seconds the swelling was stopped and the final structure was fixed by using ethanol then allowed to evaporate overnight.

After the creation of the monolayers, another alignment structure (a box shaped polytetrafluoroethylene mold), was used to put them in an ordered pile allowing layer sinteringin an ordered fashion. This time, the swelling and the neck formation were controlled using a 50/50 anisole/ethanol solution. In contrast, for randomly assembled scaffold sintering the microspheres were poured into the mold and treated with a 50/50 anisole/ethanol solution.

A) 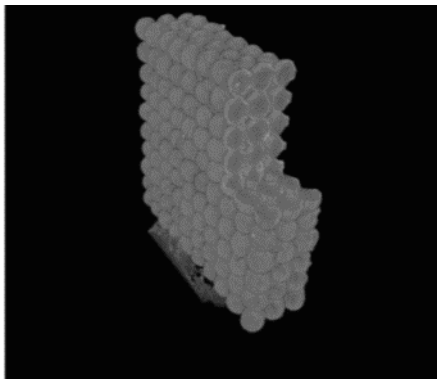 B) 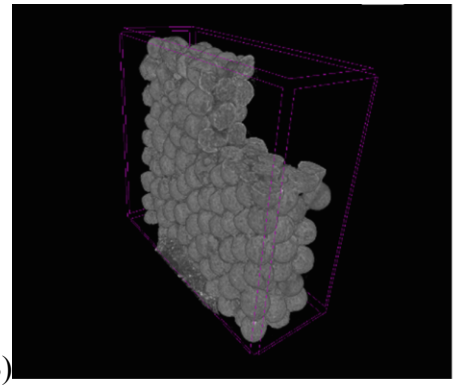

Figure 3. The figure shows the reconstructions made by SkyScan NRecon software of images acquired by a micro-CT Scan (Bruker) of orderly (panel A) and randomly (panel B) assembled scaffolds.

2.2.4 Scaffold surface treatment

Surface hydrophobicity greatly enhances the cellular response both *in vitro* and *in vivo* (31-32). However, high hydrophobicity induces a low surface wettability that negatively influences cell adhesion and proliferation. Indeed, when a cell suspension is seeded on a PCL surface it is not absorbed with a consequent slow cell growth and heterogeneous cell distribution (33).

Wettability and cell adhesion were improved in both ordered and random scaffolds via NaOH treatment by soaking the constructs in 0.1 M NaOH and ethanol (1:1) solution for 15 min at 37°C (34). This strong alkaline condition improved PCL hydrophilicity through the hydrolysis of the ester and the hydroxyl carboxylic acid groups of the polymer.

2.2.5 Water contact angle test

In order to verify the effect of the NaOH treatment we made the contact angle test. The contact angle is the angle formed by the contact of a liquid interface with a solid surface and allows to quantify the wettability of the material surface induced by a certain liquid. The measurement was performed by placing with a syringe a droplet ($\sim 2\mu$L) of deionized water on the sample surface. Droplet configuration was then captured with a camera.

The value of the contact angle was calculated as the average of the measured left and right contact angles formed between the droplet baseline and the tangent at the water/air interface. Contact angle measurements were obtained from three different regions of the surface of three samples.

2.2.6 Scaffold X-ray microtomography analysis

A qualitative analysis of scaffold structure was performed using a computerized micro-tomograph (SkyScan1172, Bruker). Micro-tomography (commonly known as CT scanning) uses X-rays to obtain projection images of 3D-objects. It quantified pores size and volume as well as the total percentage of porosity of the entire matrix.

To evaluate scaffold porosity, it is necessary to discriminate between the air and the absorbent material, corresponding to white and black points respectively. To do this, the software (SkyScan NRecon, Bruker) counted the black and white points, obtaining the ratio of the empty volume of the object and, in turn, its porosity.

2.2.7 Cell-material interaction

Human Umbilical Vein Endothelial Cells (HUVEC) (Lonza) were cultured in Human Endothelial-SFM Basal medium (Gibco) supplemented with endothelial cell growth factor (100 mg/ml) (Sigma-Aldrich), 20% foetal bovine serum (Sigma-Aldrich) and 1% Pen Strep (10,000 U/mL of penicillin G sodium and 10,000 mg/ml streptomycin sulphate in saline 0.85%) (Gibco) at 37 °C in 5% CO_2 and 100% relative humidity until they were confluent.

Afterwards we detached HUVECs by using trypsin EDTA (Lonza) and counted them. For cell adhesion assay we sterilized PCL scaffolds by UV rays before seeding 0.9×10^4cells/scaffold (n = 3 each group) in a 96-well plate. After 6 h, cells were detached and counted. To test cell-material interaction we seeded 2×10^4cells/scaffold in a 96 well plate and incubated them for 48 hours (n = 4 each group). After 3 days of incubation, scaffolds were fixed with 4% paraformaldehyde, washed 3 times with PBS and stained with phalloidin tetramethylrhodamine B isothiocyanate (Sigma-Aldrich) and Sytox green (Invitrogen) for actin microfilaments and nuclei, respectively. Cell adhesion and distribution inside the scaffold, were evaluated by a confocal Leica SP5 laser scanning microscope, equipped with a water immersion objective HCX IRAPO 25 X

0.95. For nuclei detection, samples were excited with a 488 nm argon laser, while for actin we used a 543 nm He-Ne laser. Images were processed by a Leica LAS AF software version 2.7.3.9723.

For scanning electron microscope (SEM) analysis we seeded the scaffolds (n = 3 each group) with the same number of cells. After 24 hours we fixed the cellularized constructs in 2.5% glutaraldehyde and 0.1 M sodium cacodylate at pH 7.3. Afterwards we washed the samples three times for 10 minutes in the same buffer, and then kept them on ice for 1 hour in 1% osmium tetroxide and 0.1 M sodium cacodylate at pH 7.3. We then washed the scaffolds again three times for 10 minutes in the same buffer and dehydrated them on ice in increasing concentrations of ethanol. After dehydration, we moved the samples to the critical point drying (Leica) and placed them on an aluminium stub with carbon tape before coating them with 20 nm of gold metal by sputter coating (208 HR sputter coater, Cressington). Afterwards, we observed the samples with a Zeiss Ultraplus scanning Electron microscope (35).

2.2.8 Gradient generation and sprouting angiogenesis assay

In order to study the biological response to the gradient generated by a specific growth factor we developed a device equipped with a corridor with a 100µl volume limited by glass walls where we positioned on one end the scaffold loaded with QK (40ng) as endothelial growth factor, and on the other end three spheroids at a distance of about 1cmeach other (Figure 4).

Both the scaffold and the spheroids were embedded in a three-dimensional matrix consisting of type 1 bovine collagen.

Depending on spheroid reactivity this method allowed us to assess the diffusion of the angiogenic factor in the different areas of the system and, consequently, the capacity of the scaffold to generate a spatial gradient.

After 24 hours, spheroids were fixed with 4% paraformaldehyde, stained with Sytox green (Invitrogen) and phalloidin tetramethylrhodamine B isothiocyanate (Sigma-Aldrich) and observed by a confocal microscope as described in section 1.3.7.

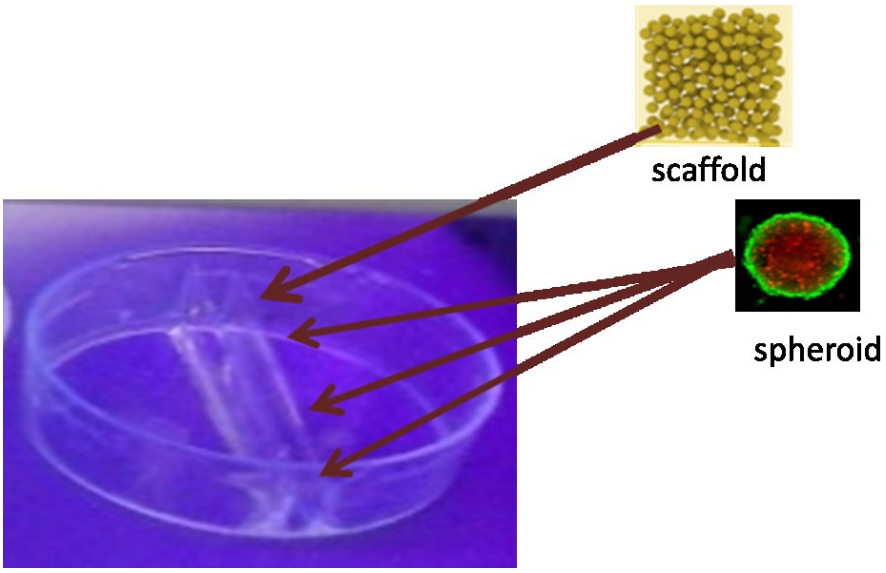

Figure 4. The image shows a petri dish modified according to our experimental setting. We made a corridor (red arrows) limited by glass walls where we positioned at the two opposite ends the matrix and the spheroids embedded in bovine collagen.

2.2.9 Scaffold implantation

Animal experiments were performed in accordance with the Directive 2010/63 / EU. All animals were housed in individual cages with free access to food and water. Male Wistar rats weighting 250-300g (n=3 each group) were divided into 2 groups and identified as OR and R for the recipients of orderly and randomly assembled scaffolds respectively.

Once anesthetized, the animals were placed in sternal decubitus. After trichotomy and disinfection with 10% Iodopovidone (Betadine®) we performed a horizontal incision of about 1 cm centrally and distally to the shoulder blades. We then performed a blunt dissection making a subcutaneous pocket of 2-3 cm.

Once positioned the scaffold inside the pocket, we sutured the skin with a 3/0 silk suture. Animals were placed on a thermal bed at 37 °C until their awakening. All the animals received antibiotic prophylaxis by enrofloxacin administration in drinking water for 3 days.

2.2.10 Histology and Immunofluorescence analyses

For both histology and immunofluorescence (IF) after euthanasia we harvested the integrated scaffolds (n = 3 each group), embedded them in OCT before snap freezingin nitrogen. Afterwards samples were cut in slices of 7 μm thickness. For histology the slices were stained with Hematoxylin-Eosin (Thermo Scientific ™) and observed by an optic microscope (Olympus BX53)

in order to evaluate the integration of the scaffold with the host tissue as well as the eventual development of a fibrous capsule around the construct.

For IF samples were processed for vessel detection and distribution. Slices were stained with mouse anti-rat antibodies for CD31 (BD Biosciences) combined with goat anti-mouse fluorescent secondary antibody Alexa Fluor 488 (Life Technologies).

The sections were examined with a fluorescence microscope (Olympus BX53) with an UPL SAPO 20 X/0.75 dry objective. The microscope was equipped with a 450-490 nm excitation filter and a 500-530 nm emission filter for Alexa Fluor 488. Images were acquired by a digital color camera (Olympus DP21) and processed by Image J software.

2.2.11 Micro-CT analysis

After euthanasia we infused 100 ml of saline solution in each animal using a syringe pump. Immediately after we infused 10 ml of Microfil®, a silicon rubber used as contrast agent for micro-CT imaging (36). After 24 hours we retrieved the scaffolds integrated with the host tissue. Explants were fixed in 10% neutral buffered formalin for at least 24 hours before micro-CT scanning (37).

2.3 Results

2.3.1 NaOH surface treatment improves hydrophilicity

PCL is a highly hydrophobic polymer so it would be naturally inadequate for cell invasion. In order to facilitate cell adhesion and proliferation we chemically treated scaffolds with NaOH. We then evaluated the efficacy of this treatment by the contact angle test.

Conventionally, if water contact angle is < 90° the solid surface is considered hydrophilic whereas if it is > 90° the solid surface is considered hydrophobic. We detected contact angle values of 104° and 64° in untreated and NaOH treated scaffolds respectively (Figure 5).

This result supports the hypothesis that NaOH treatment improves scaffolds cytocompatibility.

A) 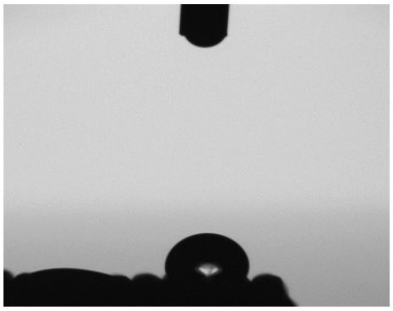 B) 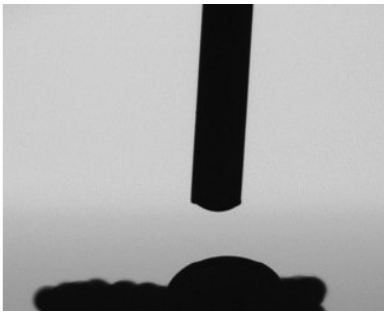

Figure 5. The figure shows scaffold hydrophilicity evaluated by the water contact angle test: in the upper part of each panel it is visible the needle used to generate the droplets. In the lower part of the panels the droplets lie on the scaffold surfaces. On the surface of the untreated scaffold (panel A) the droplet is not absorbed as it is through the surface of the NaOH treated one (panel B).

2.3.2 Bottom-up approach improves scaffold porosity

In order to evaluate scaffold porosity, we analysed micro-CT scans by NRecon software. In the reconstructed images the black and white points correspond to the void volume and to the microspheres respectively (Figure 3). Therefore, by counting the black and white points the software provides the data of interest.

The values resulting from the analysis of our samples showed a porosity of 48% in orderly assembled scaffolds versus a porosity of 40% for randomly assembled ones.

2.3.3 Cell adhesion is influenced by surface treatment but not by scaffold architecture

Cell adhesion and migration throughout the constructs were evaluated both in orderly and randomly assembled scaffolds. The cell adhesion assay didn't reveal any statistical difference between the two groups of scaffold (P>0.05), suggesting that the two different manufacturing

procedures didn't influence *in vitro* biocompatibility (Figure 6). In contrast, scaffold surface treatment with NaOH, induced a significant difference in cell behavior ($P<0.05$) as shown in the same Figure, suggesting that the improved surface hydrophilicity promotes cell adhesion.

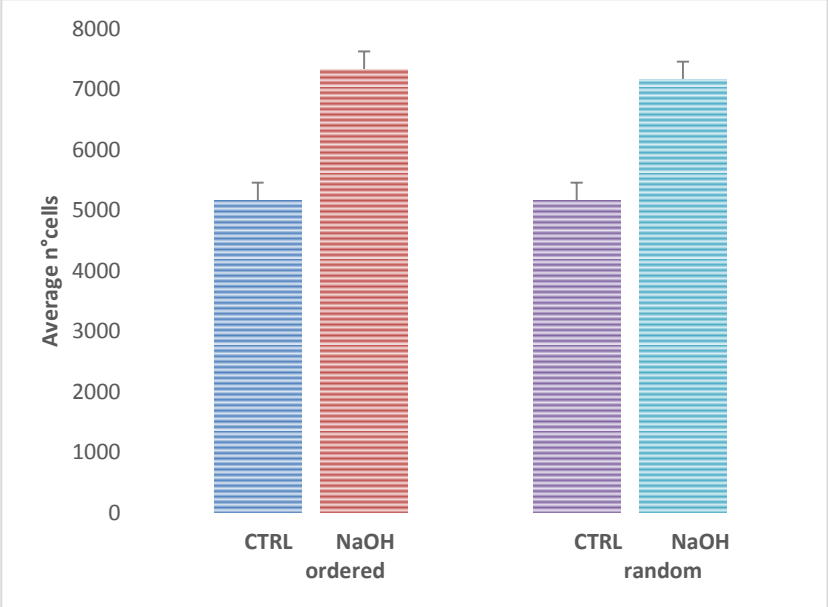

Figure 6. The graph shows the number of HUVEC cells adherent to the scaffolds after 6 hours of culture. NaOH treated scaffolds compared to untreated ones show enhanced cell adhesion while no difference is induced by the fabrication technique used to produce the orderly and randomly assembled constructs; (n = 3) ordered vs random $P>0.05$; NaOH vs untreated $P<0.05$.

2.3.4 PCL scaffolds support cell proliferation

Cell-material interaction between HUVECs and scaffolds was also analysed through confocal microscopy, by observing cell morphologyafter staining with Phalloidin tetramethylrhodamine and Sytox green chromophores after 3 days of culture. Scaffold surface, as well as its cross sections, were covered by HUVECs displaying a well-developed nucleus and cytoskeleton (Figure 7).

These results support the idea that HUVECs are able to migrate throughout the construct and not to just spread on its surface, corroborating the hypothesis that our scaffolds are reliable platforms to encourage a homogenous vascularization after implantation.

A) 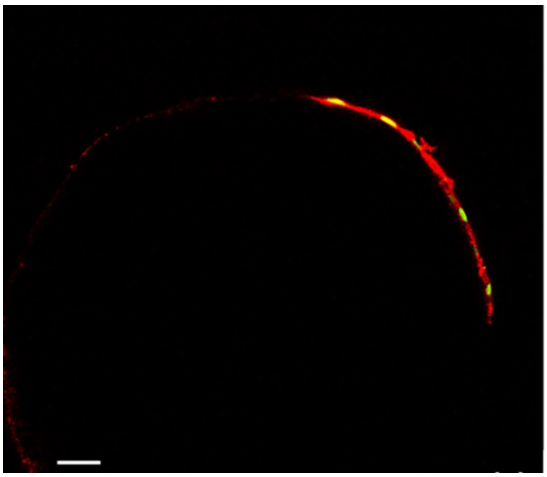 B) 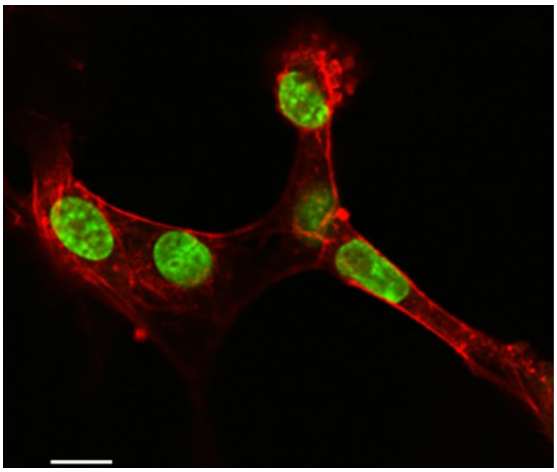

Figure 7. Confocal microscopy images of NaOH treated scaffolds acquired 3 days after cell seeding. HUVECs were stained with Sytox green and Phalloidin tetramethylrhodamine. The images are representative of 3 independent experiments (n = 3 each group) and of 10 acquisitions for each scaffold. Microspheres appear uniformly cellularized as well as the entire scaffold surface (panel A, scale bar 40 μm) and cross-section (panel B, scale bar 10 μm,25 X magnification).

2.3.5 Growth factor release from the scaffolds are able to develop a biochemical gradient

In order to investigate the ability of the scaffold to induce the development of a biochemical gradient we loaded them with QK, a peptide we used as a model molecule, which is able to act as endothelial growth factor. To this aim we performed an experiment based on the evaluation of sprouting angiogenesis in a 3D collagen matrix containing a QK loaded scaffold. More precisely, we looked at sprout formation induced by QK diffusion into the matrix.

For this purpose we modified a petri dish making a corridor, which allowed us to place both the scaffold and the spheroids linearly and to avoid the diffusion of the molecule in all directions. After 24 hours of culture we performed a quantitative analysis by counting the average number of sprouts developed from each spheroid. Spheroids were divided into 3 groups based on their distance from the scaffold.

The results showed that the scaffold generates a linear chemical gradient able to stimulate spheroid reactivity to an extent that is inversely proportional to the distance, as expected (Figure 8). In addition, the difference displayed between the groups C+ and SP1, although it is slight, may suggest that a release modulated over time could be powerful even at an early stage (24 hours).

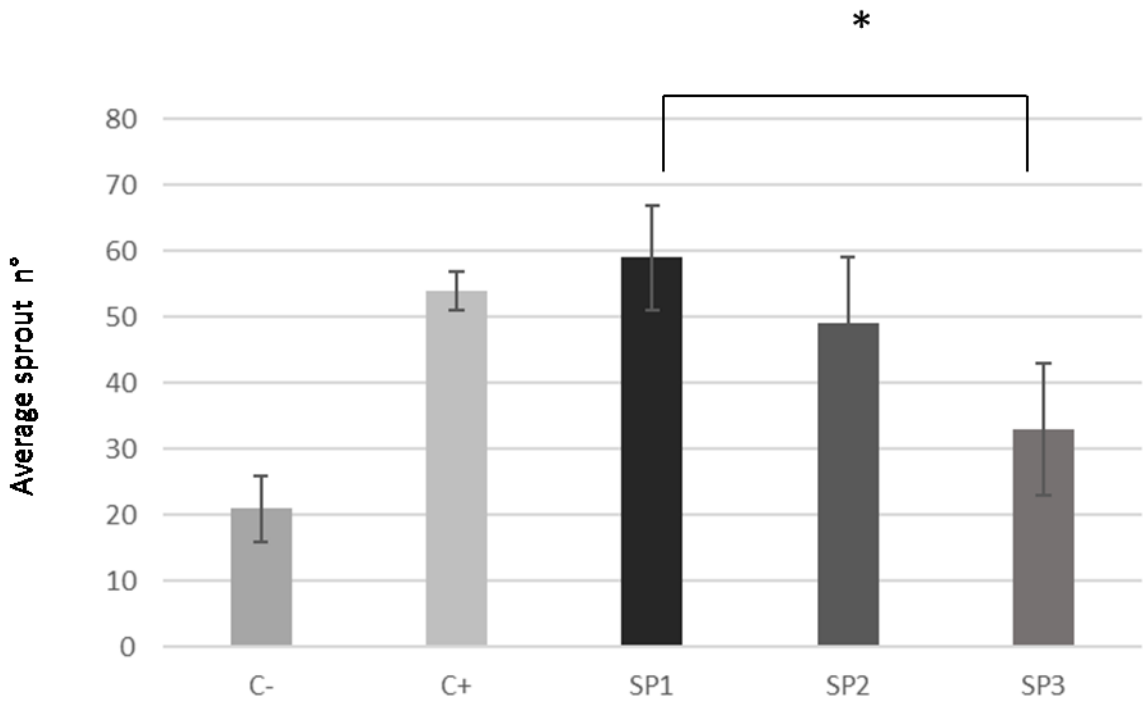

Figure 8. The graph shows spheroids reaction in response to the stimulation with 40ng/ml of QK released by the scaffold over 24 hours of culture. Reactivity was evaluated as the average number of sprouts generated from the spheroids. Spheroids belonging to the C+ group were treated with 40 ng/ml of free QK. Data are shown as mean values ± standard deviation (SD) of 3 independent experiments performed in triplicate ($p<0.05$).

2.3.6 PCL scaffolds are biocompatible

In order to evaluate the safety and the ability of the scaffold to be vascularized and integrated into the host tissue we performed a basic histological analysis through hematoxylin and eosin staining. The results showed the absence of any adverse reaction at the implantation site suggesting that the proposed scaffold is biocompatible (Figure 9).

The stained samples, indeed, didn't display any sign of encapsulation by fibrous tissue at the scaffold periphery.

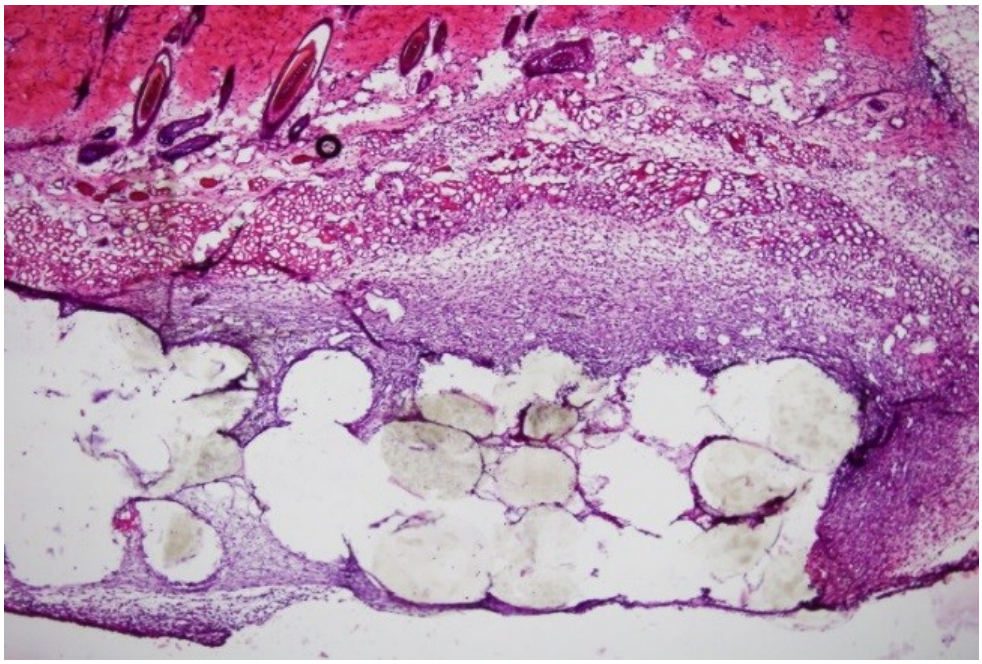

Figure 9. Image representative of samples stained by hematoxylin and eosin retrieved 7 days post-implant (n=3 each group). Scaffolds appear well integrated into the host tissue without any sign of encapsulation.

2.3.7 Orderly assembled scaffolds are able to modulate angiogenesis

Scaffold vasculogenic potential was evaluated by immunofluorescence staining with anti-CD31 antibody. We observed a difference in the extent of vessel penetration into the scaffold with a more in depth vessel infiltration in orderly assembled scaffolds versus randomly assembled ones (Figure 10).

These data corroborated the results of micro-CT analysis regarding the different suitability of the two groups of constructs to be invaded by the newly formed vessels.

A) 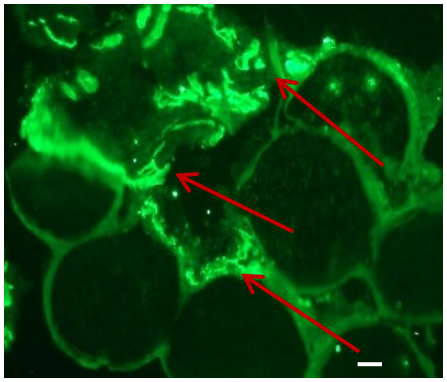 B) 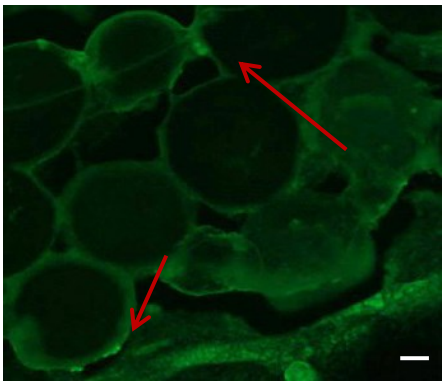

Figure 10. Images representative of Immunofluorescence staining with anti-CD31 antibody of samples retrieved 7 days post-implant (n=3 each group). The images show some vessels branching through the pores of the orderly assembled scaffold as indicated by the red arrows (Panel A scale bar 500 μm). In contrast, randomly assembled scaffold (Panel B scale bar 500 μm) appears less vascularized particularly in its inner part.

2.3.8 Orderly assembled scaffolds display a high degree of vascularization

The degree and the quality of scaffold vascularization were evaluated by analysing micro-CT data. All the samples processed were retrieved 7 days after implantation. The degree of vascularization was measured throughout the entire scaffold. The volume of the vasculature surrounding the retrieved construct was also measured, in order to differentiate the pre-existing vasculature at the site of implantation.

As "surrounding vasculature" we considered the vessels found in a volume of tissue which extension was up to 500 microns far from the scaffold surfaces (Figure 11). The total vessel volume within the orderly assembled scaffold was greater than the one reported in the randomly assembled ones.

The average percentage of the surrounding vasculature was measured as 1.8 ± 0.52% for orderly assembled scaffolds and 0.92% ± 0.79 for randomly assembled ones. In this case the statistical analysis performed by using a single factor ANOVA test did not show a significant difference between the two groups ($n = 3$, P-value>0.05), suggesting that the pre-existing vasculature at the implantation site did not affect the result.

Nevertheless, the difference concerning the surrounding vascularization is clear. Further, the distribution and the average diameter of the vessels within the scaffold were also evaluated with a

CTAn software (SkyScan). In this case, the average value is about 50 μ for both the groups. However, the percentage of the vessel number found in the orderly assembled scaffolds is 0.59 % ± 0.26 versus 0.06 % ± 0.062 of the other group suggesting that porous scaffolds with random architecture are less suitable to be invaded by larger vessels.

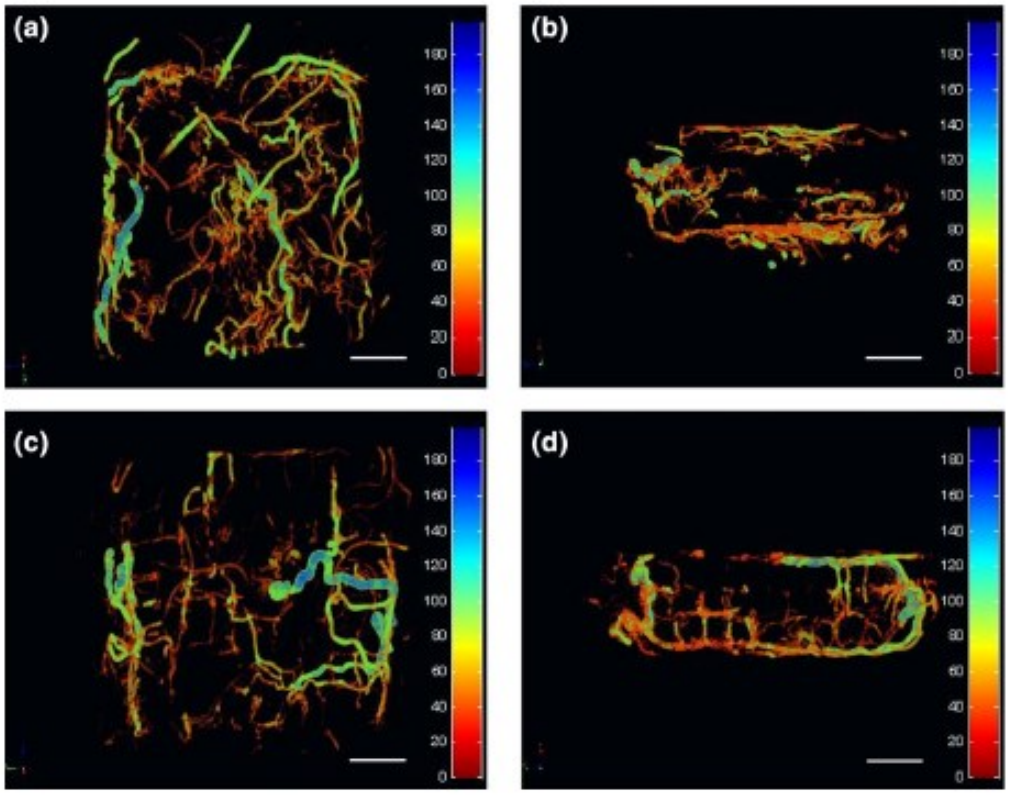

Figure 11. Micro-CT images of the newly formed vascular network 7 days after scaffold implantation. The images show that vessels mainly run around the construct surfaces in randomly assembled scaffold (Panels A, B) compared to the orderly one in which they are distributed more homogeneously (Panels C, D).

2.4 Conclusions

Establishing an adequate vascularization degree in engineered scaffolds remains a challenge in tissue-engineering. Angiogenesis, indeed, is a process of basic importance in many physiological processes, leading to the formation of a vascular network able to provide oxygen and nutrients to the newly formed tissue.

A scaffold is a biocompatible structural support, but also a construct potentially able to guide regeneration through specific physical and mechanical properties, such as a certain porosity and mechanical strength as well as the release of signal molecules. In view of this, the most recent scaffold generation includes the ability to control the release of specific growth factors.

The bottom-up PCL scaffold proposed in this work stems from the rational assembly of single units (building blocks). To this purpose we used an assembly procedure based on the solvent sintering of microspherical building blocks. The resulting product is a polymer scaffold with predefined pore size, high interconnectivity and ability to include growth factors able to control new vessel formation.

The analysis of the biological behaviour of our construct both *in vitro* and in the preclinical setting provides promising results suggesting its potential use for tissue regeneration. The data presented in the previous sections encourage us to complete the study by assaying the ability of the QK loaded scaffold to guide neovascularization after implantation. However, before starting with a new preclinical trial we plan to complete a full characterization of the release properties of our product.

References

1. Peloso A. et al., Time for organ transplantation to transition toward a regenerative medicine-focused type of research. Clin Immunol 2013; 9(10), 883–885.

2. Mount N.M. et al., Cell-based therapy technology classifications and translational challenges. Philos Trans 2015; 370(1680): 20150017.

3. Meyer U.et al., The history of tissue engineering and regenerative medicine in perspective, in Fundamentals of Tissue Engineering and Regenerative Medicine. Springer 2009, 5-12.

4. Sachlos E. et al., Making tissue engineering scaffolds work. Review Eur Cell Mater 2003; 30; 5:29-39.

5. Griffith L.G. et al., Tissue engineering current challenges and expanding opportunities. Science 2002, 295, 1009−1014.

6. Bonassar L.J. et al., Tissue engineering: the first decade and beyond. J Cell Biochem 1998, 72, 297−303.

7. Walters N.J. et al., Evolving insights in cell–matrix interactions: Elucidating how non-soluble properties of the extracellular niche direct stem cell fate. Act Bio 2014; 09.038.

8. Ventre M. et al., Determinants of Cell–Material Crosstalk at the Interface: Towards engineering of cell instructive materials. J R Soc Interface 2012; 2017−2032.

9. Ladoux et al., Physically based principles of cell adhesion mechanosensitivity in tissues. Rep Prog Phys 2012, 75, 116601.

10. Bengt K. et al., Material-tissue Interfaces: The Role of Surface Properties and Processes. Environ Health. Perspect 1994; 102, 5:41-45

11. Chiu LL., Scaffolds with covalently immobilized VEGF and Angiopoietin-1 for vascularization of engineered tissues. Biomaterials 2010; 31:226–241.

12. Colpo P. et al., Surface functionalization for protein and cell patterning. Adv Biochem Eng Biotechnol 2010; 117:109-30.

13. Zarana S.P. et al., Angiogenesis with biomaterial-based drug- and cell-delivery systems J. Biomater. Sci Polymer Edn 2004; 701–726.

14. Collier J.H. et al., Synthesis and characterization of polypyrrole–hyaluronic acid composite biomaterials for tissue engineering applications. Biomed Mater Res 2000; 50, 574.

15. Bose S. et al. Bandyopadhyay, Recent advances in bone tissue engineering scaffolds. Trends in Biotechnol 2012; 30(10): p. 546-554.

16. Clapp et al., Peptide Hormone Regulation of Angiogenesis. Physiol Rev 2009; 89: 1177–1215.

17.Ferrara N. et al., Role of vascular endothelial growth factor in the regulation of angiogenesis. Kidney International 1999; pp. 794–814

18. Dreier et al., Early responses of vascular endothelial cells to topographic, A J Physiol 2013; C290-C298.

19. Vilches et al., Cell-surface interaction in biomedical implants assessed bysimultaneous fluorescence and reflection confocal microscopy. Microsc Res Tech 2007; 70, 361

20. Kuddannaya S., et al., Surface chemical modification of poly(dimethylsiloxane) for the enhanced adhesion and proliferation of mesenchymal stem cells. ACS Appl Mater Interfaces 2013; 5(19):9777–84.

21. Liekens S. et al.,.Angiogenesis: regulators and clinical application. Biochem Pharmacol 2001; 61(3):253-70

22. Carmeliet P., Mechanisms of angiogenesis and arteriogenesis. Nat Med 2000; 6(4):389–95.

23. Bouhadir K.H. et al., Promoting Angiogenesis in Engineered Tissues. J Drug Target 2001; 9(6):397-406

24. Wood J.A., et al., Biophysical Cueing and Vascular Endothelial Cell Behavior. Materials 2010, 3(3), 1620-1639

25. Hoanget D. al., Fabrication of Hyalunonan-Poly (Vinylphosphonic Acid)-Chitosan Hydrogel for Wound Healing Application. Science 1985; 228, 1324.

26. Shivani S. et al., Delivery of VEGF using Collagen-coated Polycaprolactone Scaffolds Stimulate Angiogenesis. Biomed Mater Res A 2012; 100(3): 720–727.

27. Cleland J.L. et al., A. Development of poly-(d,l-lactide-coglycolide) microsphere formulations containing recombinant human vascular endothelial growth factor to promote local angiogenesis. J Control Release 2001; 72:13–24.

28. Luciani A. et al., PCL microspheres based functional scaffolds by bottom-up approach with predefined microstructural properties and release profiles. Biomaterials 2008; 29(36):4800–7.

28. Luciani A. et al., Solvent and melting induced microspheres sintering techniques: a comparative study of morphology and mechanical properties. J Mater Sci Mater Med 2011; 22(9):2019–28.

29. Bordes C. et al., Determination of poly(epsilon-caprolactone) solubility parameters: application to solvent substitution in a microencapsulation process. Int J Pharm 2010; 383(1–2):236–43.

30. Goddard et al., Polymer surface modification for the attachment of bioactive compounds. Progress in Polymer Science 2007; 32(7): 98-725.

31. Xu L.C. et al., Effects of surface wettability and contact time on protein adhesion to biomaterial surfaces. Biomaterials 2007; 28(22): p. 3273-83.

32. Yeo A et al., Surface modification of PCL-TCP scaffolds improve interfacial mechanical interlock and enhance early bone formation: an in vitro and in vivo characterization. J Biomed Mater Res A 2010; 92(1):311–21.

33. Hanson A.D. et al., Effects of oxygen plasma treatment on adipose-derived human mesenchymal stem cell adherence to poly (L-lactic acid) scaffolds. J Biomater Sci Polym Ed 2007; 18(11): 1387-400.

34. Rossi L. et al., Vasculogenic potential evaluation of bottom-up, PCL scaffolds guiding early angiogenesis in tissue regeneration J Mater Sci Mater Med 2016; 27:10.

35. Bonassar L. J. et al., Tissue engineering: the first decade and beyond. J Cell Biochem 1998, 72, 297−303.

36. Downey C. et al., Ex-Vivo Micro-Computed Tomographic Imaging of Blood Vessels and Necrotic Regions within Tumors. PLoS One 2012; 7(7): e41685.

37. Vasquez SX et al., Optimization of microCT imaging and blood vessel diameter quantitation of preclinical specimen vasculature with radiopaque polymer injection medium. PLoS One 2011; 6(4): e19099.

Chapter 3

Modulation of topographical signals to guide directional sprouting

3.1 Introduction

3.1.1 Biochemical and biomechanical cues

Angiogenesis is a process that requires the coordination of different cellular events originating from different signals such as hypoxia and inflammation (1). Endothelial cells (ECs) are particularly influenced by signals coming from the extracellular matrix (ECM) and from the basal membrane, which are both rich in topographical cues (2). These signals start a cascade of events promoting different cellular processes like migration, proliferation, tubulogenesis and phenotype determination. All these events are related to the interaction between the integrins, which are proteins situated on the outer surface of the cell membrane, and the ECM ligands such as fibronectin and laminin (Figure. 1).

In some pathological conditions, this sequence of events can be altered or absent. In addition, revascularization is often too slow or limited to the surface layers, resulting in inadequate supply of O_2 and nutrients (3). In this context, all these aspects are of basic importance to create tissue engineered constructs able to resemble the natural characteristics of the ECM (4).

Biomaterials used as three-dimensional matrices for the cells are named “scaffolds”. Therefore, a scaffold represents the extracellular environment that supports cell growth, proliferation and differentiation during tissue and organ regeneration. In addition, it temporarily replaces the mechanical function of the natural ECM, gradually degrading in order to be replaced by the newly synthesized one.

Properly designed porous scaffolds are able to encourage the formation of a functional vascular network, however the newly formed vessels are generally irregular and tortuous. This irregularity provokes blood flow alterations with the consequent increase of vascular permeability and blood clot formation. For this reasons the spatial and temporal control over the network formation remains an open challenge in this field, being the generation of a functional vasculature essential for the development of well-organized tissues (5).

Therefore, tissue engineering currently aims to the dynamic control of vascular network formation through the use of new materials and the set-up of new strategies. Contact guidance is the process through which cells respond to the specific structural arrangement of the surrounding microenvironment, modifying their shape but also their migration direction according to it (6).

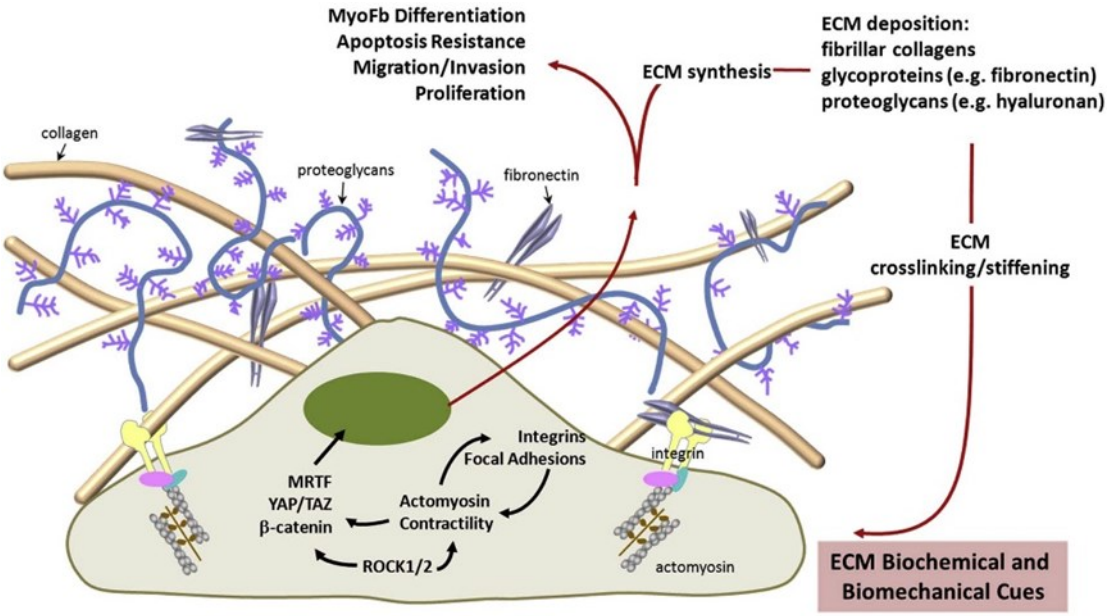

Figure 1. The image depicts the complexity of the signals involved in the cell-matrix interplay. Biochemical and biomechanical stimuli derived from the ECM trigger intracellular signals through multiple pathways. These signals are also able to direct cell differentiation and, therefore, to influence cell phenotype *(Thannickal V.J. et al. Am J Pathol 2014, 184: 1643e1651).*

3.1.2 Topographic signal influences cell behaviour

The cell-substrate interplay is critical in several cellular mechanisms. Singhvi et al. demonstrated the influence of topographical signals on endothelial cell behaviour through the use of patterned substrates, that are able to mimic the topographic features of the ECM (6). An intrinsic property of ECs is their capacity to exert mechanical forces on the external environment. These forces can modify the mechanical and structural features of the matrix that, in turn, activates feedback responses able to regulate the different cell functions. Collagen and fibrin, indeed, are often used to induce network formation *in vitro.* In fact, as reported by Lesman and colleagues they both form fibrillar interconnected structures that can be highly remodelled also showing unique physical properties (7).

These tubules follow the direction of collagen fibers that have previously been aligned by EC traction forces. Further, when external forces elongate this fibrillar gel, tubules alignment follows the same direction, suggesting that the forces induced by vessel formation are sufficient to cause a far-reaching deformation inside the gel (8). Therefore, it seems clear how cells communicate through the substrate deformation caused by cell traction forces.

Several studies show that the mechanical stiffness of the environment directly influences the formation of tubule-like structures in both 2D and 3D cultures based on fibrin and collagen gels (8). Deroanne and co-workers showed, for example, that the different degree of collagen stiffness results in morphology and phenotype modifications revealing that rigid structures discourage tubule formation (6).

3.1.3 Sprout formation during angiogenesis

As described in Chapter 1, tubulogenesis requires the coordination of many events involving cytoskelethon, actin, microtubules, and integrins, which expression is regulated by the rigidity of the ECM. Shen at al. revealed that the reduced adhesion between ECs and the extracellular matrix improves vascular network organization. In addition, Fisher et al. showed that myosin II inhibits blood vessels branching, so that its local diminution increases sprout formation.

Over the past few years several models based on cells combined with biomaterials allowed the study of vessel branching mechanisms *in vitro*. De Mel et al., indeed, showed that the

application of mechanical forces to the cells as well as the control of their internal tension influences tubule organization and orientation (9). However, a more in-depth comprehension of the mechanisms that underlie these phenomena is mandatory to support the generation of a clinically relevant vascular network (7).

3.1.4 How a pattern can influence cell behaviour

Once explained the impact of the microenvironment on cell function, in order to support and direct cell growth it has to be understood how the 3D structure of a biomaterial should be and how its modification may influence cell behaviour. To this purpose different protocols have been developed over the past decade. The majority of them are based on the contact guidance of the 3D matrix, but none of them is able to recapitulate the dynamic behaviour of the natural ECM (9).

Among the *in vitro* models, we chose a sprouting angiogenesis assay based on the use of spheroids made of human umbilical vein endothelial cells (HUVECs). This assay, indeed, holds the following advantages:

- is relatively fast and widely accepted
- mimics the physiological processes better than a standard 2D culture
- shows the different cellular properties (adhesion, proliferation, migration) involved in the process
- allows the observation of both spheroid core and branching tubules (10).

In our work, we first analysed sprouting angiogenesis in a "semi-3D" environment represented by a bottom-patterned cell culture plate. We defined this environment as "semi-3D" because collagen does not embed the spheroids but just covers them. Contemporarily, in order to understand the role of the dynamical change of the topographical signal in the early-stage of sprouting angiogenesis we chose a 2D platform made up of a photosensitive polymer, named poly (Disperse Red 1 methacrylate). This polymer, composed of azobenzenes, is able to modify its surface shape following the application of a light stimulus (11).

Azobenzenes are molecules able to absorb light at a specific wavelength (514 nm in our case) and to modify their geometry through trans-cis-trans isomerization. This feature can be exploited to draw a variety of patterns through the exposure of the polymer to a laser beam of a

confocal microscope. This method, that may be defined “single-laser-beam technique”, allows a real-time patterning together with the imaging of the consequent cell behaviour (12).

3.2 Materials and methods

3.2.1 Writable single-well system

Commercial poly (Disperse Red 1 methacrylate) (pDR1m) (Sigma-Aldrich) was dissolved in chloroform (5% w/v) and then deposed onto a glass coverslip (15 mm diameter) through spin coating technique. A custom-made well plate system with azopolymers at the bottom of each well was built. A polystyrene empty cylinder of 10 mm internal diameter was glued on each well with a UV-based polyurethane polymer membrane, named Norland optical adhesive (NOA63) (Figure2). NOA is a light-cured polymer that is widely used in soft lithography and in many other laboratory practices

A) 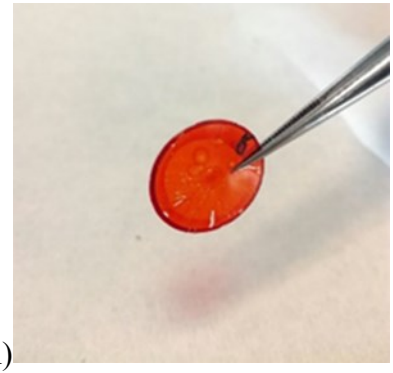 B) 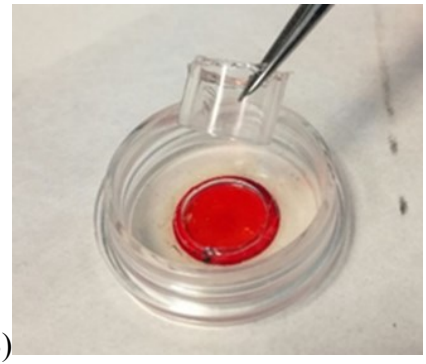 C) 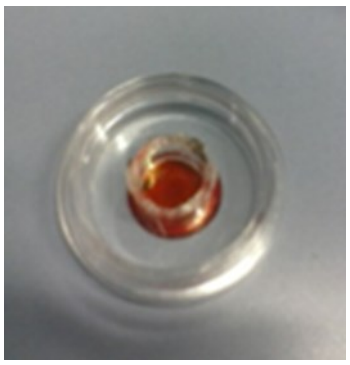

Figure 2. The image shows how we prepared the single-well custom-made system. Firstly, we glued a glass slide coated with the polymer (panel A) on the perforated bottom of a p35 petri dish (panel B). Secondarily we made the walls of the well by gluing on the bottom of the petri dish the walls of a standard 48 well cell culture plate (panel C).

3.2.2 NOA pre-patterned single-well system

Pre-patterned single wells were produced using NOA. A NOA patterned substrate is obtained by UV polymerization of a NOA coated surface enlightened at 365 nm wavelength for 20

minutes. After that, the patterned substrate is glued to the bottom of the well as previously described.

3.2.3 Cell culture and generation of endothelial spheroids

Human Umbilical Vein Endothelial Cells (HUVECs) (Lonza) were grown in Medium 200 supplemented with LSGS kit (Life-Technologies) at 37 °C in 5% CO_2 and 100% relative humidity. Cells were seeded into tissue culture flasks and cultured until they reached confluence. To generate endothelial spheroids, they were used at early passages (II-IV).

After 3-4 days of culture, confluent HUVEC monolayers were trypsinized and 800 cells/spheroid were suspended in culture medium containing 0.25 (w/v) carboxymethylcellulose (Sigma), seeded into ultra-low-attachment u-bottom 96-well plates (Costar) and cultured to allow spheroid formation (13).

3.2.4 Sprouting angiogenesis assay on patterned surfaces

After 24h of culture, spheroids were harvested and centrifuged at 900 rpm for 15 min. Then, 1-2 spheroids each time were seeded on a polymer coated glass slide (single-well system). Afterwards, they were covered with 1.2 mg/ml of bovine skin collagen. After collagen polymerization, M200 culture medium, supplemented with LSGS kit (Life-Technologies) and Hepes 25 μl/ml (Sigma) was added into the single-well system.

Polymer surface was then photo-patterned by using a Leica SP5 confocal microscope with an Argon laser set at 514 nm wavelength. Rectangular regions of interests (ROI) have been drawn, with a spacing of 2 μm, directly underneath each spheroid (14). Spheroids belonging to the control group were seeded in the same conditions on a glass slide without the polymer. Samples, prepared in triplicates, were left in the incubator overnight and imaged by an inverted microscope the day after.

Spheroids were then fixed in 4% paraformaldehyde (PFA) and stained for imaging with Sytox green (Invitrogen) and phalloidin tetramethylrhodamine B isothiocyanate (Sigma-Aldrich) in order to be observed by a Leica SP5 confocal laser scanning microscope, equipped with a water immersion objective. For the study that included static patterned surfaces both spheroids and collagen fibers were imaged through a multiphoton microscope (TCP SP5 multiphoton, Leica

Microsystems). Collagen images were acquired by using the second harmonic generation (SHG) technique.

3.2.5 Pattern writing simulation

In order to ascertain that was not the laser that influenced sprout orientation, the spheroids were seeded in standard conditions in a common well-plate or on a bare glass. After collagen polymerization, we simulated the pattern writing as previously described. Afterwards, spheroids were incubated overnight.

3.3 Results

3.3.1 Surfaces patterned by single-laser-beam technique influence sprout orientation

The evaluation of sprouting orientation made by confocal microscope showed that sprouts were mostly aligned along the pattern direction, while the spheroid cores acquired a polarized shape (Figure 3). On the contrary, when cultured in standard conditions in a common plate or on a bare glass, spheroids developed isotropic tubules, while their cores maintained a rounded morphology. Moreover, we noticed a high remodelling of the collagen along the axis of the patterned matrix around both the spheroid cores and ramifications, suggesting that cell activity in those regions was intense.

To check whether the material was really influencing sprouting, we performed a time-lapse imaging using a confocal microscope after pattern inscription. These videos showed an increased cell activity after patterning, with the following change of sprout direction (Figure 4).

A) 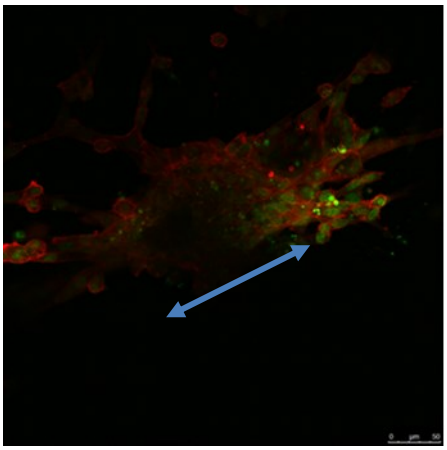 B) 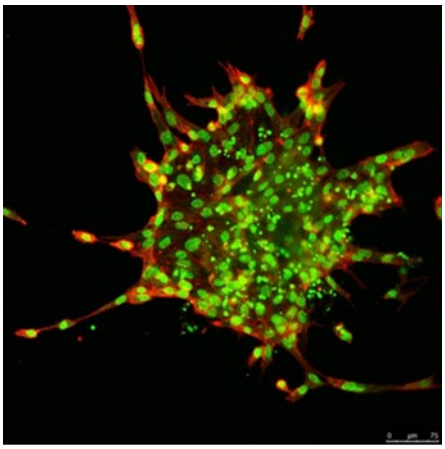

Figure 3. Confocal microscopy images of HUVEC spheroids acquired 24h after seeding. Spheroids were stained with Sytox green and Phalloidin. Images are representative of 3 independent experiments performed in triplicate. Panel (A shows sprout development following the direction of the pattern (blue arrow), in contrast with the isotropic tubules developed by the spheroids of the control group (Panel B).

A) 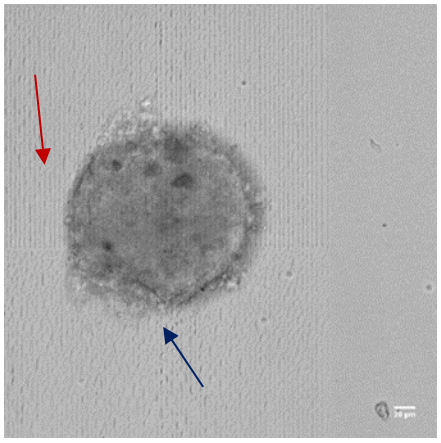 B) 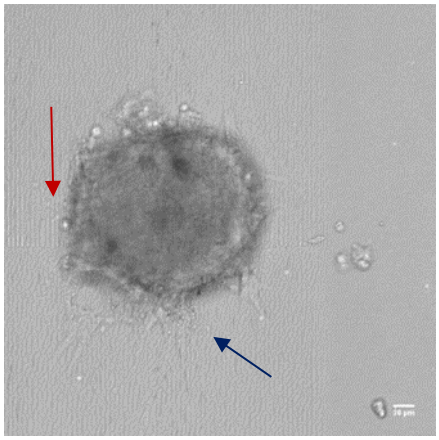

Figure 4. Images taken from a time lapse video of a HUVEC spheroid seeded on pDR1m polymer. Panel A) corresponds to a spheroid imaged right after pattern inscription, while panel B) corresponds to the same spheroid imaged 132 minutes later. Red arrows indicate pattern direction, while blue arrows indicate the modified position of the sprout in response to the pattern.

3.3.2 Effect of static patterns on sprout alignment

Lin et al. support the hypothesis that fibrillar matrices such as collagen or fibrin gels influence cell orientation. To exclude the possibility that sprouts followed the signal from the

fibrillar matrix and not the one from the inscribed pattern, we observed collagen organization by second harmonic generation (SHG) imaging technique using a multiphoton microscope.

For this study, we designed a static pattern with a specific material, the Norland optical adhesive (NOA). When we tested spheroid behaviour on a NOA pre-patterned surface we saw that even in this case, as happened when the pattern was written after spheroid seeding, the sprouts elongated in the pattern direction.

Furthermore, we noticed that collagen remodelling made by the sprouts is more intense around them (Figure 5) supporting our hypothesis that is the pattern and not the collagen fibers laying on the pre-patterned polymer to influence sprout direction.

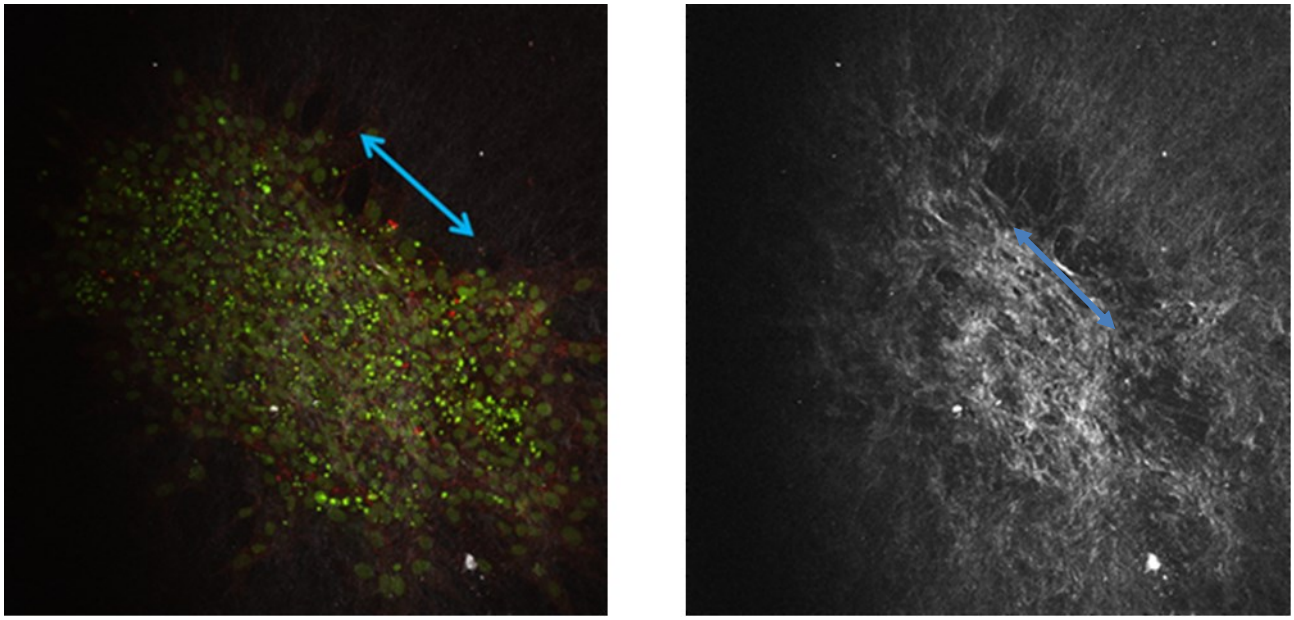

Figure 5. Multiphoton microscopy images of HUVEC spheroids acquired 24h after the seeding on a NOA static pattern. As shown in panel (A both the spheroid core and the sprouts are elongated following the direction of the pattern. Panel B) displays collagen organization remodelled by the sprouts imaged by second harmonic generation technique. In both panels the blue arrow indicates the direction of the pattern.

3.3.3 Laser illumination does not influence spheroid behaviour

To assess whether the laser light affects sprouts directional orientation, we simulated the pattern inscription by pointing the laser on the standard plate that contained the spheroids exactly as we did when we draw the pattern underneath them.

The images acquired by a confocal microscope show that 24 hours after illumination with the single-laser-beam technique spheroids developed isotropic sprouts, while their cores maintained a rounded morphology (Figure 5). This finding allowed us to exclude a direct role of laser illumination in the development of aligned sprouts.

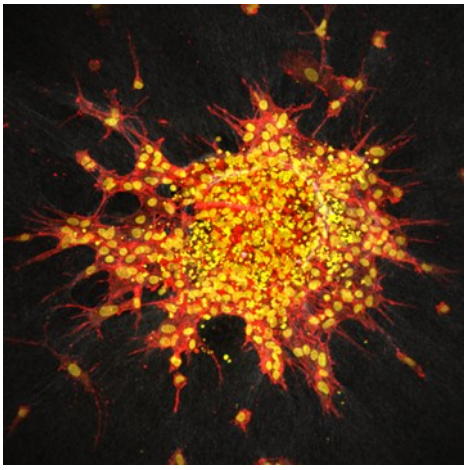

Figure 6. Confocal microscopy image representative of spheroid behaviour 24h afterillumination with a single-laser-beam. Spheroids were stained with Sytox green and Phalloidin. The picture shows that there is no influence of laser illumination on sprout orientation.

3.4 Conclusions

Understanding cell behaviour in response to external environmental stimuli is central to tissue engineering. Nowadays, an increasing number of studies investigate cell aptitude in following the physical characteristics, in particular topography, of the culture substrate.

This concept becomes critical when extended to cells as functional units of tissues and organs, switching from the culture plate to the body. In this work we looked at the influence of

dynamic topographic signals on sprouting angiogenesis but also at the possibility to exert a potential space-time control.

To test our hypothesis, we performed an angiogenesis assay based on the use of spheroids composed of human vein endothelial umbilical cells. We made the topographic signal by using poly (Disperse Red 1 methacrylate) (pDR1m), that is a polymer able to change its surface profile when illuminated.

We showed that the topographic signal we can write on the polymer surface is able to influence cell behaviour. In particular, we observed that spheroid sprouts were mostly aligned along the pattern direction, while their cores acquired a polarized shape. In contrast, spheroids belonging to the control group developed isotropic tubules with the cores featured by a standard rounded morphology.

Collectively, these data support our hypothesis that the platform we developed may be used as a reliable tool to investigate what physiologically happens to the cells when their microenvironment undergoes dynamic topographic modifications.

References

1. Martin-Saavedra F. M. et al., Temporal and spatial patterning of transgene expression by near-infrared irradiation. Biomaterials 2014; 35(28): 8134–8143.

2. Gasiorowski J Z. et al., Alterations in Gene Expression of Human Vascular Endothelial Cells Associated with Nanotopographic Cues. Biomaterials 2010; 31(34): 8882–8888.

3. Martin-Saavedra F. M, et al., Spatiotemporal Control of Vascular Endothelial Growth Factor Expression Using a Heat-Shock-Activated, Rapamycin-Dependent. Gene Switch. Hum Gene Ther Methods 2013; 24:160–170.

4. Khan O.F. et al., Endothelialized biomaterials for tissue engineering applicationsin vivo. Trends Biotechnol 2011; 29 (8): 379-387.

5. Liliensiek S.J. et al., Modulation of Human Vascular Endothelial Cell Behaviours by Nanotopographic Cues. Biomaterials 2010; 31(20): 5418–5426.

6. Singhvi R. et al., Effects of substratum morphology on cell physiology. Biotechnol Bioeng 1994; 43:764−771.

7. Lesman A. et al., Mechanical regulation of vascular network formation in engineered matrices. Adv Drug Deliv Rev. 2016; 15; 96:176-182.

8. Nikkhah M. et al., Directed endothelial cell morphogenesis in micropatterned gelatin methacrylate hydrogels. Biomaterials 2012; 33(35):9009-9018.

9. De Mel et al. Biofunctionalization of Biomaterials for Accelerated in Situ Endothelialization A Review. American Chemical Society 2008; 9 (11): 2969-2979.

10. Bourget J.M. et al., Recent Advances in the Development of Tissue-engineered Vascular Media Made by Self-assembly. Procedia Engineering 2013; 59:201 – 205

11. Blacher S. et al., Cell Invasion in the Spheroid Sprouting Assay: A Spatial Organisation Analysis Adaptable to Cell Behaviour. PLoS One 2014; 9(5): e97019.

12. Priimagi A. et al., Azopolymer-based micro- and nanopatterning for photonic applications, J Polym Sci Pol Phys 2013, 52, 163–182.

13. Borselli C. et al., Bioactivation of collagen matrices through sustained VEGF release from PLGA microspheres. J. Biomed Mater Res 2010. A 92A, 94–102.

14. Rianna C. et al. Spatio-Temporal Control of Dynamic Topographic Patterns on Azopolymers for Cell Culture Applications. Adv Funct Mater 2016, 26, 7572–7580

15. Lin L. et al., Microfluidic alignment of collagen fibers for in vitro cell culture. BioMed Microdevices 2006; 8(1): 35-41.

Chapter 4

Controlled delivery of Carbon Monoxide from PLGA nanoparticles for liver regeneration

4.1 Introduction

4.1.1 Liver regenerative ability

The liver performs many physiological key functions such as to defend the body against toxic chemicals absorbed through foods; to secrete essential proteins, for example albumin and the majority of coagulation factors; to storage glycogen, which is an important energy reserve and to regulate the levels of ammonia enabling the brain function (1). Last but not least, liver is able to return to its original mass after a resection or an injury thanks to its ability to regenerate (1).

In case of partial hepatectomy (PHTx) hepatocyte mitosis begins within 24-48 hours after the end of the surgical procedure. Afterwards, the remnant liver becomes hypertrophic in order to compensate the removed volume and the impaired organ function (2). Liver resection is rarely performed in patients with liver cirrhosis, in fact it is known that in this case liver regeneration is severely compromised. There is extensive literature on liver regeneration after PHx in "normal" liver, while fibrotic organ regeneration remains understudied (2).

Transplantation is often the only treatment available, however it is limited by the shortage of organ donors and by the potential post-operative liver failure (3). Alternatives to liver transplantation have been studied but they cannot be applied to the clinical practice due to several hindrances. In fact, decellularized scaffolds can be damaged by the reagents used during the procedure while polymer scaffolds and extracorporeal bioartificial liver fail to provide sufficient nutrients and O_2 supplies (4). Although the widespread interest in the field, effective therapies to promote the regeneration of a damaged liver have not been found yet (5).

In view of these considerations, preclinical studies focused on the development of new approaches for liver regeneration are crucial. The most commonly used experimental model of liver injury is the partial hepatectomy (PHx). After PHx, up to 95% of the hepatocytes start to replicate in order to compensate the activity of the lost tissue; the residual liver increases its volume until the original liver mass has been replaced (2).

4.1.3 CO-releasing molecules

The literature reports CO ability to stimulate cell replication and, therefore, to modulate hepatocyte (HCs) proliferation during regeneration (3).
CO use in the clinic, however, still suffers from several unsolved issues such as the difficulties related to its dosage when administered by inhalation together with the inadequate local delivery, low bioavailability and poor water solubility (6-7).

In view of the above-mentioned features of CO there is a growing interest in the development of molecules able to release it in a controlled fashion. In this perspective the potential of the so-called CO-releasing molecules (CORMs), discovered by Motterlini et al. is huge (8). These compounds are generally transition metal carbonyls that display the same pharmacological activity of the gas, including vessel relaxation, attenuation of coronary vasoconstriction and suppression of acute hypertension. However, their use in the clinical practice is hampered by some intrinsic characteristics. For example, CORM-1 (dimanganese decacarbonyl) and CORM-2 (tricarbonyldichlororuthenium(II)) besides the inclusion of transition metals in their molecules are soluble only in organic solvents and release CO very quickly (few minutes). In contrast, CORM-3 (Tricarbonylchloro (glycinato) ruthenium(II)) is soluble in water but it still releases CO too fast. Further, CORM-A1 (sodium boranocarbonate) does not contains metals, is soluble in water and releases CO slower than the other CORMS but, as shown in Figure 2, still too rapidly (9).

In this scenario the goal of our work is the maintenance of therapeutic levels of CO in the blood through a controlled release of CORMs from engineered nanoparticles.

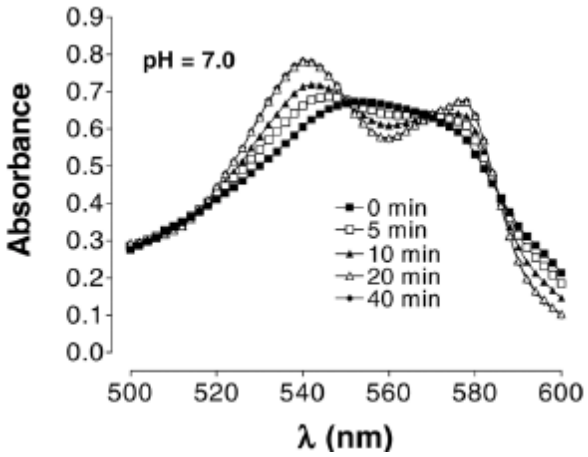

Figure 2. The graph shows the release curves of CO from CORM-A1. Release kinetics were made using the conversion rate of myoglobin (Mb) into deoxy-myoglobin (MbCO). CO binding to Mb was monitored over time by measuring the changes in the absorption spectra *(Motterlini et al., FASEB J 10.1096/fj.04-2169fje).*

4.1.4 Poly (lactic-co-glycolic acid) is a good candidate for nanoparticle fabrication

In general CO intracellular delivery from CORMs is difficult due to the low solubility and cellular uptake of these molecules. Many research groups are currently involved in the development of the ideal carrier for CORMs transport and release.

We chose the FDA-approved polymer poly (lactic-co-glycolic acid) (PLGA) to fabricate our nanoparticles (NPs). PLGA is widely used thanks to the possibility to control the release kinetic of any encapsulated molecule by playing with its degradation time.

In addition, varying the molecular weight of the polymer and modifying the ratio between poly-lactic acid and glycolic acid, one can modulate PLGA physical properties and degradation kinetics. In particular, PLGA degradation rate can be accelerated by increasing its hydrophilicity which is generally required when a short-term release (up to 1 month) is desirable. For a long-term release (1-6 months), it is more appropriate to consider the choice of a polymer with low hydrophilicity.

Furthermore, PLGA is featured by a high versatility since it can be used to fabricate micro and nano-carriers as well as prosthesis with a thickness of some millimeters. These carriers are able to vehiculate a wide range of molecules such as drugs, peptides or proteins (Figure 3).

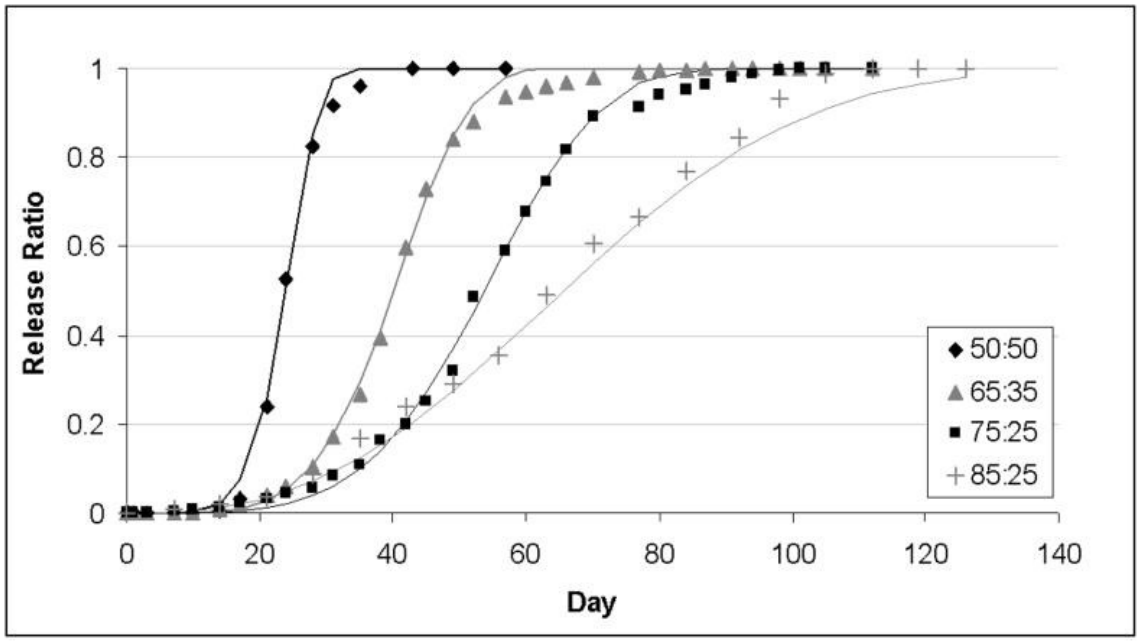

Figure 3. In vivo degradation profiles for 50:50, 65:35, 75:25 and 85:15 of the poly (lactic-co-glycolic acid) (PLGA) . Note that 65:35 PLGA means that the 65% of the copolymer is lactic acid and the 35% is glycolic acid. *(Makadia et al.; Polymers 2011; 3(3): 1377–1397).*

4.2 Materials and methods

4.2.1 Hepatic resection model (70%)

According to approved institutional animal care and use committee (IACUC) protocols we used male CD-1 mice of 6-8 weeks of age, weighing 25-35 gr to reproduce a 70% hepatectomy model. Animals were anesthetized with isoflurane, after skin sanitization we made a blunt dissection of the abdominal skin and muscles and then an incision to expose the liver. Afterwards we placed and tied a 2-0 non absorbable suture as closest as possible to the base of the left lateral lobe of the liver (Figure 4). we then resected the liver 2-3 mm away from the knot. The same procedure was repeated for both the right lateral and the median lobes. We then sutured the peritoneum and the skin with a 4-0 Vicryl absorbable suture (10).

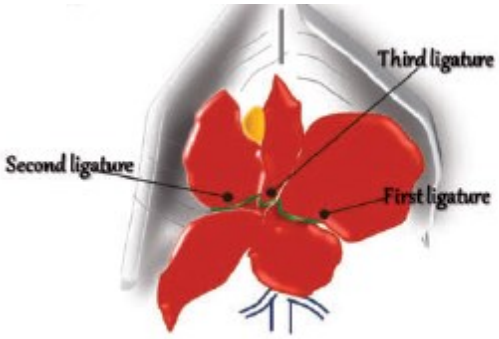

Figure 4. The figure shows how to place the ligatures for an optimal ligation of the three lobes of the liver that have to be removed for a 70% liver resection *(Y.A. Nevzorova et al., J Lab Anim 2015; 49(S1) 81–88).*

4.2.2 Production of poly (lactic-co-glycolic acid) nanoparticles

Poly lactic-co-glycolic acid (PLGA) (Resomer RG 504H, Evonik, Germany) nanoparticles were prepared according to the double nanoemulsion technique (11). Briefly, 20 mg of PLGA (75:25) were dissolved in ethyl acetate (EA) and 100 µl of a solution of rohodamine 6G (Sigma-Aldrich) in water (1mg/ml) were added. The latter mixture was emulsified by vortexing for 5 minutes.

The resulting emulsion was then sonicated using a probe sonifier (Qsonica) for 30 sec at amplitude 2 (primary nanoemulsion). This primary nanoemulsion was immediately poured into 3 ml of 1% (w/v) aqueous Pluronic F68 (Sigma-Aldrich), and then sonicated for 120 sec at Amplitude 1 (secondary nanoemulsion). The resulted double nanoemulsion was then poured into 7 ml of water and stirred overnight to allow the evaporation of the organic phase.

Finally, nanoparticles were washed and collected using Amicon ultra-4 centrifuge tubes (10 kDa, Millipore) (15' 4°C 5000 rpm). NPs were then filtered using 0.22 µm filters.

4.2.3 Cryo-TEM analysis of PLGA nanoparticles

Nanoparticle morphology was observed by cryo-TEM (transmission electron microscope). In particular, frozen hydrated samples were prepared by applying a 3 µl aliquot to a previously glow-discharged 200 mesh holey carbon grid (Ted Pella, USA). Before plunging into nitrogen

cooled liquid propane, the grid was blotted for 1.5 sec in a chamber at a temperature of 4 °C and a humidity of 90% using a FEI Vitrobot Mark IV (FEI company, the Netherlands).

The particles were imaged using a Tecnai G2 F20 transmission electron microscope (FEI company, the Netherland) equipped with a Shotky field emission gun operating at an acceleration voltage of 200 kV and recorded at low dose with a 2k x 2k Ultrascan CCD camera (Gatan, USA).

4.2.4 Nanoparticle characterization

We made a qualitative evaluation of NP size distribution and polydispersity index (PDI) by dynamic light scattering (DLS). During DLS analysis a laser illuminates the sample and the intensity of the scattered light variation is measured. NP movement generates the intensity variation measured by the detector.

The size of our NPs was <100 nm and the PDI was 0.164; the graph also shows that nanoparticles were well dispersed as demonstrated by the single peak of the curve <100 nm (Figure 5). NP morphology was assessed by cryogenic transmission electron microscopy (cryo-TEM) that is the technique generally used to study size, shape and internal structure of nanoparticulate carrier systems (Figure 6).

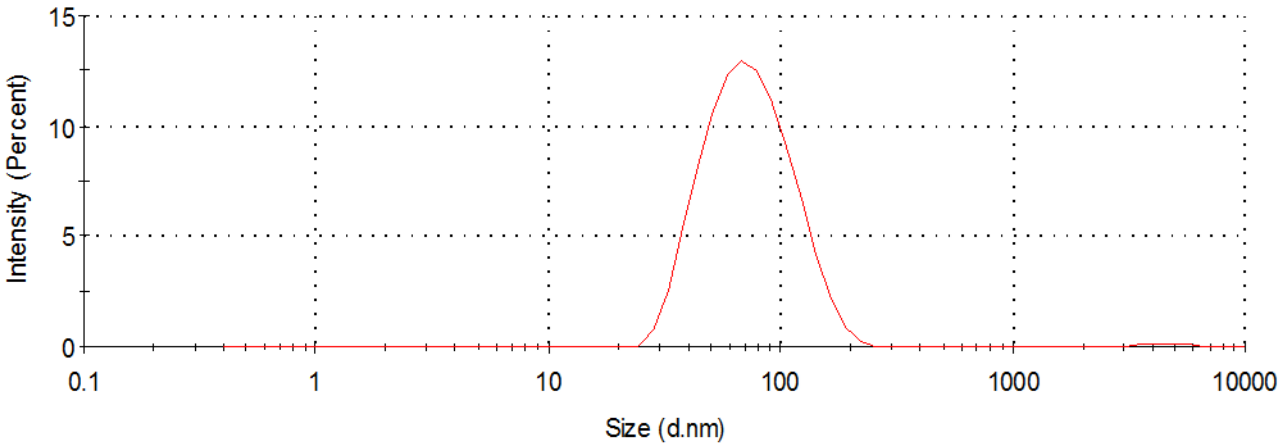

Figure 5. The graph displays the sizes range of PLGA nanoparticles measured with dynamic light scattering. The single peak of the curve shows that nanoparticles are well dispersed.

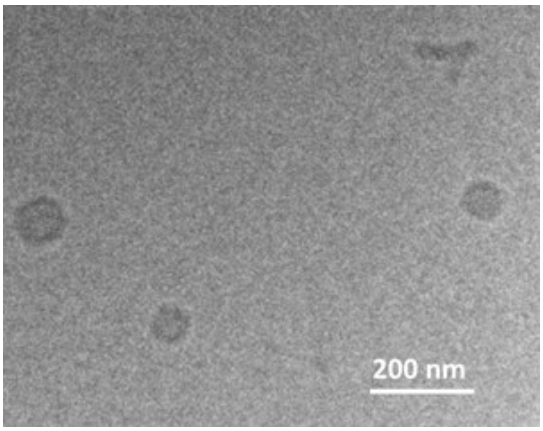

Figure 6. The picture shows a cryogenic transmission electron microscopy image of PLGA nanoparticles (NPs). The NPs displayed are intact and homogeneously rounded.

4.2.5 Nanoparticle infusion into the portal vein

To infuse the NPs into the portal vein mice were anesthetized with isoflurane. After skin sanitization we did a blunt dissection and then an incision of skin and abdominal muscles, afterwards we identified and exposed the portal vein. Briefly a dose of 15mg/kg of NPs suspended in a volume of 100 µl was infused into the vein with a 1ml syringe (12). At the end of the infusion the discontinued tissues were sutured with a Vicryl 4/0 absorbable suture.

4.3 Results

4.3.1 PLGA nanoparticles fabricated with the double emulsion technique are safe

Before loading the NPs with CORMs we tested their safety by administering them through the portal vein. We then evaluated liver reaction by measuring ALT levels in the blood at different time points (1 hour, 3 and 7 days).

When measured 1 hour after the infusion, ALT were higher in treated mice than in the untreated ones, probably because of the transient injury induced by the increased pressure into the portal vein during the infusion.

After 3 days, indeed, the value returned to the baseline and so was maintained until the last endpoint. This result guarantees that our PLGA nanoparticles fabricated by using the double emulsion technique can be safely administered by intraportal infusion (Figure 7).

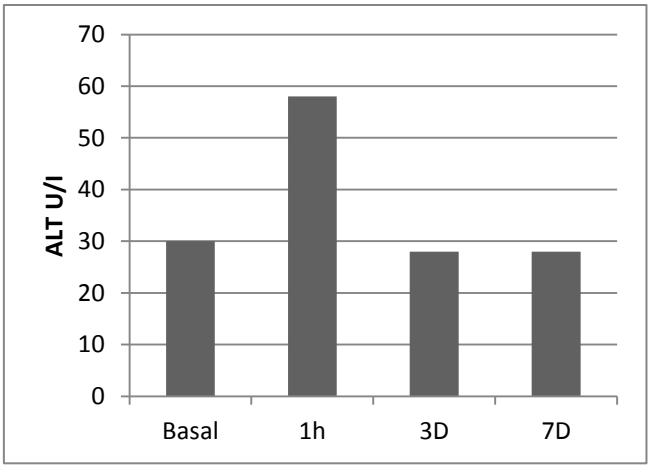

Figure 7. Blood levels of ALT measured 1 hour and 3 and 7 days after nanoparticle administration. The graph shows that the infusion of PLGA nanoparticles through the portal vein do not damage the organ.

4.4 Conclusions

Several studies revealed the positive effects of CO in the restoration of organ functions (liver, kidney, heart and others) after injury, however this molecule is still considered mostly a toxic gas.

In addition, CO therapeutic use is hampered by the difficulty to modulate its administration. CO, indeed, is slightly soluble in water so that to reach therapeutic concentrations it should be inhaled at high doses becoming, therefore, dangerous.

These issues have been partially overcome through the introduction of the so-called CO-releasing molecules (CORMs). These compounds are able to release CO in the blood, nevertheless, the release of the gas is still too fast for therapeutic applications.

In this context we are testing the hypothesis that by encapsulating CORMs in polymer nanoparticles we will be able to vehiculate and release them, and in turn CO, in a controlled manner. We chose a model of liver regeneration because of our past experience with studies focused on the investigation of the regenerative ability of CO after liver ischemia/reperfusion injury (13).

The data presented in this chapter, although very partial, encourage us to test the ability of CORM loaded nanoparticles to enhance liver regeneration.

References

1. Michalopoulos G. et al., Liver Regeneration. J Cell Physiol 2007; 213(2): 286–300.
2. Kuramitsu K. et al., Failure of Fibrotic Liver Regeneration in Mice Is Linked to a Severe Fibrogenic Response Driven by Hepatic Progenitor Cell Activation. Am J Patho 2013 Vol. 183.
3. Kuramitsu K. at al., Carbon Monoxide Enhances Early Liver Regeneration in Mice after Hepatectomy. Hepatol 2011; 53(6): 2016–2026.
4. Mazza G. at al., Decellularized human liver as a natural 3D-scaffold for liver bioengineering and transplantation. Scientific Reports 2015; 5:13079.
5. Yuan-Sheng L. at al., Cells and Materials for Liver Tissue Engineering Cell. Transplantation 2013; 685-700
6. Heinemann SH. at al., Carbon monoxide – physiology, detection and controlled release. Chem Commun. 2014; 50(28): 3644–3660.
7. Zuckerbraun BS. et al., Carbon monoxide protects against liver failure through nitric oxide-induced heme oxygenase 1. J Exp Med 2003; 198(11):1707-16.
8. Motterlini R. et al., Bioactivity and pharmacological actions of carbon monoxide-releasing molecules. Curr Pharm Des 2003;9(30):2525-2539
9. Motterlini R. et al., CORM-A1: a new pharmacologically active carbon monoxide-releasing molecule. FASEB Journal 2004; 10.1096/fj.04-2169fje
10. Nevzorova YA. et al., Partial hepatectomy in mice. Lab Ani. 2015; 49(S1) 81–88
11. Yang L. et al. Biodistribution Studies of Nanoparticles Using Fluorescence Imaging: A Qualitative or Quantitative Method? Pharm Res 2012, 29(12): 3273–3277.
12. Lacey C. at al., The effect of nanoparticle properties, detection method, delivery route and animal model on poly(lactic-co-glycolic) acid nanoparticles biodistribution in mice and rats. Drug Metab 2013; 1-15.
13. Andria B. at al., Biliverdin protects against liver ischemia reperfusion injury in swine. PLoS One 2013; 8(7): e69972.